

## SHEAR LAG APPROXIMATION OF SOLUTIONS OF NEARLY UNIDIRECTIONAL PROBLEMS IN ELASTIC MEDIA

M. LUTCHANSKY† and L. M. SLAVIN†

Bell Telephone Laboratories, Incorporated  
Whippany, New Jersey

**Abstract**—A simple mathematical model similar to one which has been used in shear lag analyses and to describe the continuum limit of a multilayer sandwich material is suitable for obtaining estimates of solutions to problems in isotropic elasticity if it can be assumed that the stress or strain distribution is nearly unidirectional. The model is applied to the case of an end-loaded cantilever beam in which warping of the cross section is prevented at the support. The transverse deflections predicted are in close agreement with the results of Euler–Bernoulli theory with an added shear contribution, and in regions away from the support the axial stress distribution follows a linear variation. However, intricate end effects are predicted near the support with stress intensification at the outer fibers. These end effects become negligible a short distance away from the support, in agreement with Saint-Venant's principle.

### INTRODUCTION

A MATHEMATICAL model is obtained from the two-dimensional equations of isotropic elasticity by assuming in one direction, either zero normal stress or zero normal strain. The governing equations are similar to those for both the continuum limit of a multilayer composite medium and particular orthotropic elastic media. This model is suggested as a simple tool for obtaining approximate solutions to certain problems in isotropic elastic media where the stress or strain distribution may be nearly unidirectional. The zero normal strain assumption is the basis for the shear lag model developed by Hildebrand [1] and the approximate method of von Kármán and Chien [2] for treating problems of torsion with variable twist. The present discussion indicates that the range of applicability of such simplifications includes a wider class of problems. Although these simplifications are not new, they have not been popularized for the type of problem discussed herein. It is felt that because they may be of considerable usefulness, their properties should be more fully investigated.

The model consists of a Laplace-type equation for displacements in the direction of the essential normal stresses and a total equilibrium equation in the transverse direction. That a similar model describes a multilayer sandwich beam when the number of layers is large and the layer spacing is uniform was demonstrated by Tarnopolskii, *et al.* [3]. It was noted in [1, 3] that the behavior of a particular orthotropic medium is also governed by this model. Although the discussion in this paper centers on the two dimensional case, similar treatment can be applied to certain three dimensional problems.

The model is applied here to the case of an isotropic elastic end-loaded thin rectangular cantilever beam in which warping of the cross section is prevented at the built-in end

† Member of Technical Staff.

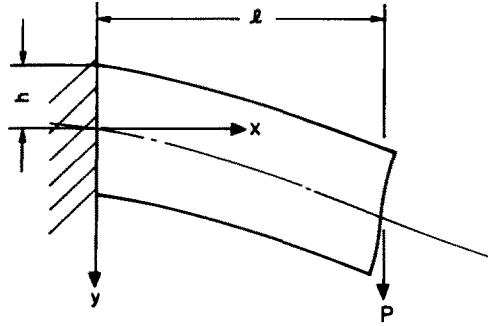


FIG. 1. Cantilever beam with warping prevented at the support.

(Fig. 1). Intricate end effects at the support are predicted with stress intensification at the outer fibers.

**SIMPLIFICATION OF EQUATIONS OF ELASTICITY**

The Navier equilibrium equations for plane stress with body forces neglected can be written

$$\frac{\partial}{\partial x} \left[ \frac{E}{(1-\nu^2)} \left( \frac{\partial u}{\partial x} + \nu \frac{\partial v}{\partial y} \right) \right] + \frac{\partial}{\partial y} \left[ G \left( \frac{\partial u}{\partial y} + \frac{\partial v}{\partial x} \right) \right] = 0 \tag{1}$$

and

$$\frac{\partial}{\partial y} \left[ \frac{E}{(1-\nu^2)} \left( \frac{\partial v}{\partial y} + \nu \frac{\partial u}{\partial x} \right) \right] + \frac{\partial}{\partial x} \left[ G \left( \frac{\partial u}{\partial y} + \frac{\partial v}{\partial x} \right) \right] = 0 \tag{2}$$

where  $E$  is Young's modulus,  $\nu$  is Poisson's ratio,  $G$  is the shear modulus and standard notation has been used for the other quantities.

For the case  $\nu = 0$  the assumptions  $\sigma_y = 0$  and  $\epsilon_y = 0$  are identical and imply that  $v = v(x)$ . Equations (1) and (2) simplify to

$$\frac{\partial^2 u}{\partial x^2} + \frac{G}{E} \frac{\partial^2 u}{\partial y^2} = 0 \tag{3}$$

and

$$G \frac{\partial}{\partial x} \left( \frac{\partial u}{\partial y} + \frac{dv}{dx} \right) = 0. \tag{4}$$

For a problem in which  $v$  actually does depend on  $y$  to a small degree the effect of the term neglected in (1) may be assumed small relative to the effects of the other terms retained whereas the effect of the simplification of (2) which results in (4) imposes a severe restriction. Indeed (4) implies that the shear stress must be independent of  $x$  which in turn restricts the  $\sigma_x$  stress variations to be linear in  $x$ .

For the beam then, a total equilibrium equation in place of (4) is less restrictive. That total equilibrium is consistent with the assumption of zero transverse strain can be readily seen by the use of the principle of minimum potential energy. For the end-loaded beam the potential energy,  $\pi$ , under the present restrictions can be written

$$\pi = \frac{1}{2} \int \int \int_V \left[ E \left( \frac{\partial u}{\partial x} \right)^2 + G \left( \frac{\partial u}{\partial y} + \frac{dv}{dx} \right)^2 \right] dV - Pv(l)$$

where  $P$  is the end load which we will assume is distributed over the free end in an ideal parabolic manner. Minimization of  $\pi$ , keeping in mind that  $v = v(x)$ , leads to the field equation (3) and the total equilibrium equation for a beam of unit width

$$\frac{\partial}{\partial x} \int_{-h}^h \left( \frac{\partial u}{\partial y} + \frac{dv}{dx} \right) dy = 0 \tag{5}$$

along the beam with the corresponding boundary conditions

$$u = v = 0 \quad \text{at} \quad x = 0, \tag{i}$$

$$\frac{\partial u}{\partial y} + \frac{dv}{dx} = 0 \quad \text{at} \quad y = \pm h, \tag{ii}$$

$$\frac{\partial u}{\partial x} = 0 \quad \text{at} \quad x = l, \tag{iii}$$

and

$$\int_{-h}^h \left( \frac{\partial u}{\partial y} + \frac{dv}{dx} \right) dy = \frac{P}{G} \quad \text{at} \quad x = l. \tag{iv}$$

For the more general case where  $v \neq 0$ , the assumption  $\sigma_y = 0$  reduces (1) to

$$\frac{\partial^2 u}{\partial x^2} + \frac{1}{2+v} \frac{\partial^2 u}{\partial y^2} = 0 \tag{6}$$

while the assumption  $\varepsilon_y = 0$  reduces (1) to

$$\frac{\partial^2 u}{\partial x^2} + \frac{(1-v)}{2} \frac{\partial^2 u}{\partial y^2} = 0. \tag{7}$$

For two dimensional problems the model, then, consists of the modified Laplace equation such as (3), a total equilibrium equation such as (5)†, together with a suitable set of boundary conditions for a given problem.

### CANTILEVER BEAM SOLUTIONS

The solution for the cantilever beam example for the case  $v = 0$  is obtained by a straightforward separation of variables procedure. We find

$$v = \sum_{n=0}^{\infty} a_n \sqrt{(E/G)} [\cos(\lambda_n x) - 1] \cosh \sqrt{(E/G)} \lambda_n h, \tag{8}$$

$$u = \sum_{n=0}^{\infty} a_n \sin \lambda_n x \sinh \sqrt{(E/G)} \lambda_n y, \tag{9}$$

† More generally, with a distributed loading  $q(x)$  per unit length along the top or bottom surface of the beam the total equilibrium equation (5) is replaced by

$$\frac{\partial}{\partial x} \int_{-h}^h \left( \frac{\partial u}{\partial y} + \frac{\partial v}{\partial x} \right) dy = \frac{q}{G} \tag{5a}$$

along the beam.

and a corresponding axial stress distribution

$$\sigma_x = E \frac{\partial u}{\partial x} = E \sum_{n=0}^{\infty} a_n \lambda_n \cos \lambda_n x \sinh \sqrt{(E/G)\lambda_n} y \quad (10)$$

where

$$\lambda_n = \frac{(2n+1)}{2l}, \quad n = 0, 1, 2, \dots, \quad (11)$$

and

$$a_n = \frac{1}{lG\lambda_n(\sinh \sqrt{(E/G)\lambda_n} h - \sqrt{(E/G)\lambda_n} h \cosh \sqrt{(E/G)\lambda_n} h)}. \quad (12)$$

The stress expression (10) converges at all points except where the outer fibers meet the wall. There the series is properly divergent for finite  $G$  indicating a singularity†. For infinite  $G$  the distribution reduces to the linear one of Euler–Bernoulli theory. That the exact theory of elasticity predicts a singularity at the corners of a cantilever whose built-in end is completely fixed is indicated by Williams' results [5].

An alternate form of the solution can be obtained using moment equilibrium and axial force equilibrium at all  $x$  in place of (ii) as the two sets of conditions are interchangeable. In this procedure the  $u$  field is determined completely without simultaneously finding  $v$ . Hence the model, in a sense, decouples  $u$  and  $v$ .

For nonzero Poisson's ratio, assuming  $\sigma_y = 0$ ,  $v = v(x, y)$  and the model will indicate an unrealistic lateral expansion and contraction at the built-in end as in the Saint-Venant cantilever solution. As in the previous case, here

$$\sigma_x = E \frac{\partial u}{\partial x}. \quad (13)$$

Using the moment and axial force equilibrium conditions in place of (ii), and solving (6) we find

$$u = \sum_{n=0}^{\infty} a_n \sin \lambda_n x \sinh \lambda_n \sqrt{(2+\nu)} y \quad (14)$$

where  $\lambda_n$  is given by (11) and

$$a_n = \left( \frac{2+\nu}{2+2\nu} \right) \frac{P}{lG\lambda_n[\sinh \sqrt{(2+\nu)\lambda_n} h - \sqrt{(2+\nu)\lambda_n} h \cosh \sqrt{(2+\nu)\lambda_n} h]}. \quad (15)$$

With little difficulty it is found for this case that

$$v = -\nu \sum_{n=0}^{\infty} \frac{1}{\sqrt{(2+\nu)}} a_n \cos \lambda_n x \cosh \lambda_n \sqrt{(2+\nu)} y + \frac{2(1+\nu)}{(2+\nu)h} \sum_{n=0}^{\infty} \frac{a_n}{\lambda_n} [\cos(\lambda_n x) - 1] \sinh[\lambda_n \sqrt{(2+\nu)} h] + \frac{Px}{2Gh}. \quad (16)$$

† The divergence of (10) at the corners can be shown by subtracting the divergent series

$$\mp \frac{P\sqrt{(E/G)}}{\pi h} \sum_{n=0}^{\infty} \frac{1}{(n+1)}$$

from (10) and showing the convergence of the resulting expression using Raabe's test [4].

The solution of (7) for the assumption  $\epsilon_y = 0$  is of the same form as obtained in the previous cases :

$$u = \sum_{n=0}^{\infty} a_n \sin \lambda_n x \sinh \sqrt{\left[\frac{2}{(1-\nu)}\right]} \lambda_n y, \tag{17}$$

where  $a_n$  is given by (12) with  $E/G$  replaced by  $2/(1-\nu)$ . Here

$$v(x) = \sqrt{\left[\frac{2}{(1-\nu)}\right]} \sum_{n=0}^{\infty} a_n [\cos(\lambda_n x) - 1] \cosh \sqrt{\left[\frac{2}{(1-\nu)}\right]} \lambda_n h \tag{18}$$

with the axial stress given by

$$\sigma_x = \frac{E}{(1-\nu^2)} \frac{\partial u}{\partial x}. \tag{19}$$

### NUMERICAL RESULTS

For all computations, the value of  $P/2hE$  was taken to be  $\frac{1}{6} \times 10^{-4}$ . To study the effects of beam length variations the parameter  $\eta \equiv l/h$  was given the values 2, 4 and 10. Poisson's ratios of zero and 0.3 were considered.

In Fig. 2 the stress intensification is exhibited for the case  $\nu = 0, \eta = 2, \sigma_y = 0$ . The upper curve represents the stress along a fiber whose position is  $y = 0.995h$  and the upper dashed line represents the corresponding linear stress distribution value for that fiber. Note that  $\bar{x} = x/l$  and  $\bar{y} = y/h$ .

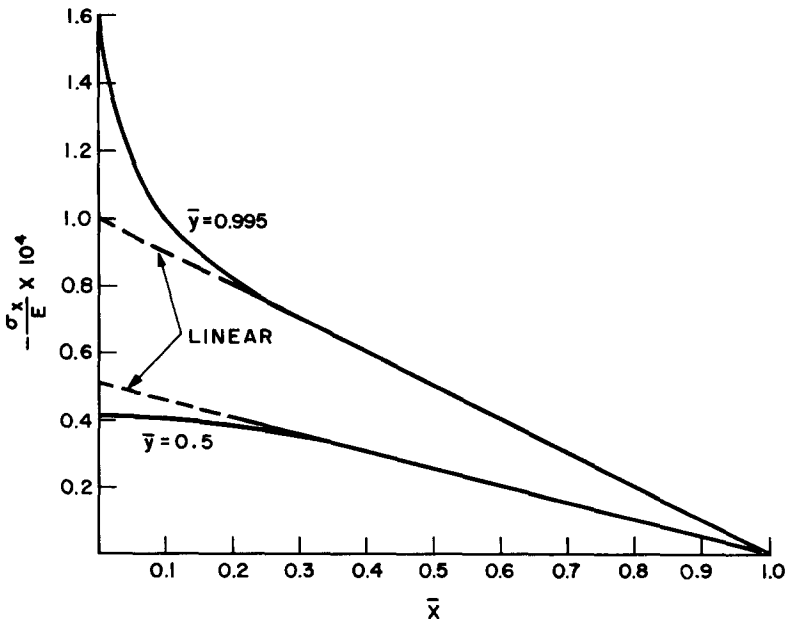


FIG. 2. Stress variation with axial position ( $\sigma_y = 0$ )  $\eta = 2, \nu = 0$ .

In Figs. 3-5 the stress distributions through the depth are shown for various cross sections. It can be seen that the effect of varying Poisson's ratio is of secondary importance, with the curves lying very close to one another. Comparing these cases it is seen that as a percentage of the length of the beam, the nonlinearity of the stress distribution extends further from the wall the shorter the beam. However as a percentage of the depth the extension of the wall disturbance into the beam is about the same for all beams. This can best be demonstrated by studying the variation of the  $\gamma_{xy}$  distribution.

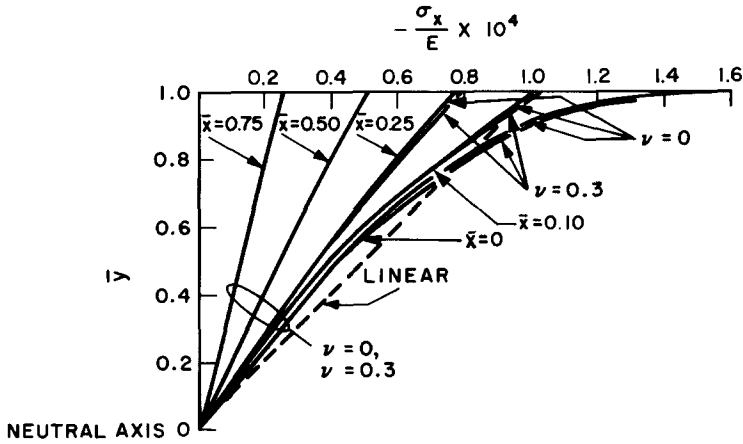


FIG. 3. Stress variation through depth ( $\sigma_y = 0$ ) $\eta = 2$ .

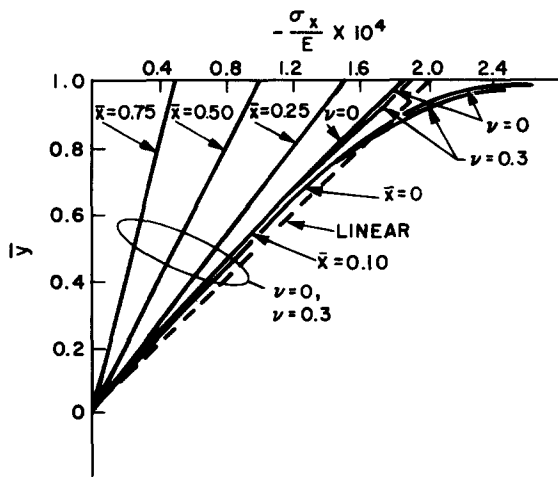


FIG. 4. Stress variation through depth ( $\sigma_y = 0$ ) $\eta = 4$ .

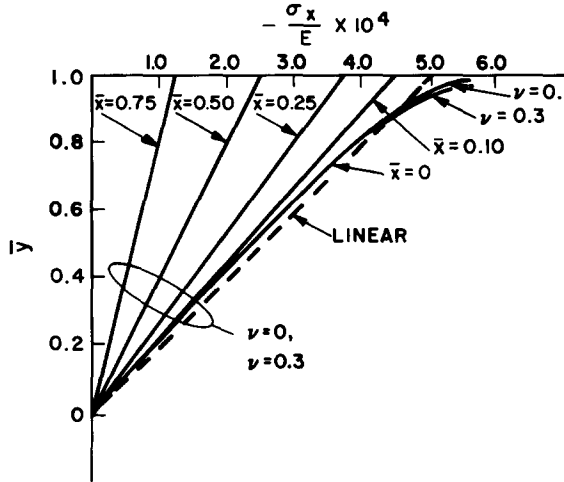


FIG. 5. Stress variation through depth ( $\sigma_y = 0$ )  $\eta = 10$ .

In Fig. 6 it is seen that near the wall there is a transition in the shear strain distribution from rectangular through the depth to parabolic. In Fig. 7 we have plotted the ratio of the shear strain along the central fiber to its value at the wall. The upper curve is for  $\nu = 0$  and it can be seen that this curve also is modified only slightly by variations in  $\nu$ . For all values of  $\eta$ , essentially the same curve applies if we use abscissae scaled as shown. Thus it is seen that for beams of various lengths the shear stress distribution changes from rectangular

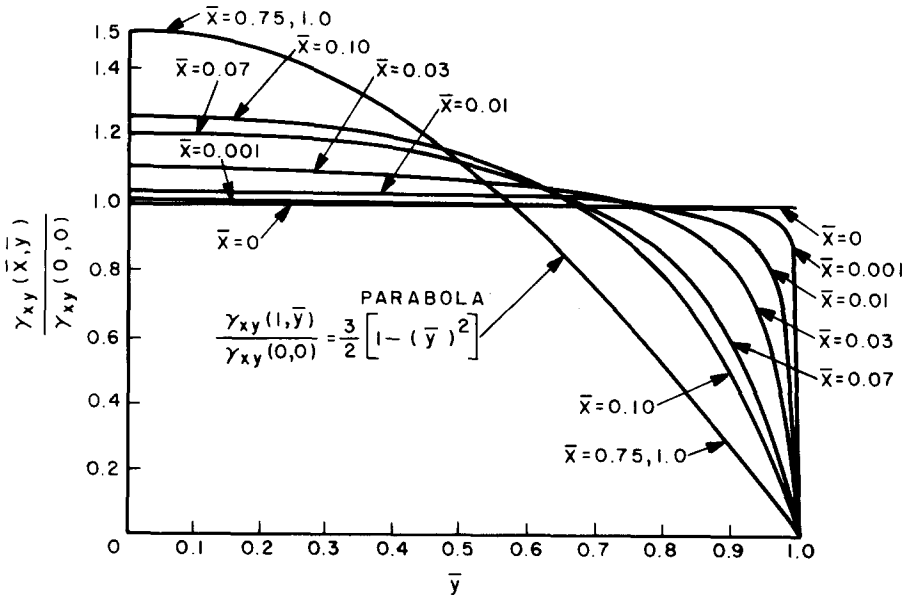


FIG. 6. Shear strain distribution variation near wall ( $\sigma_y = 0$ ),  $\nu = 0$ ,  $\eta = 2$ .

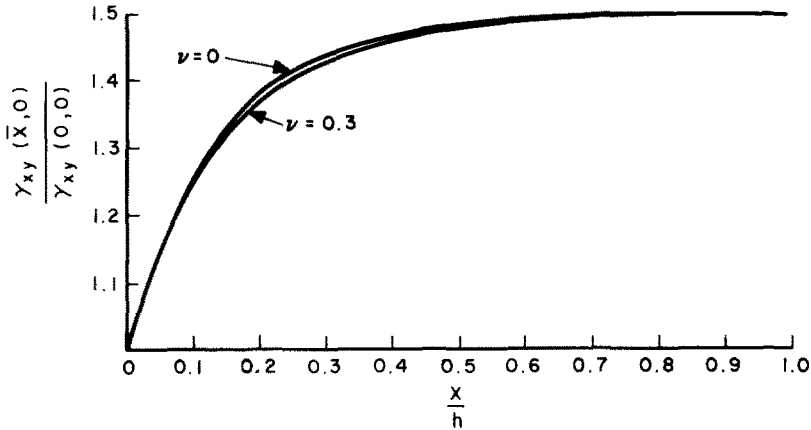


FIG. 7. Variation in shear strain along the length for neutral axis ( $\sigma_y = 0$ ).

to parabolic within a distance comparable to the depth of the beam. The  $\gamma_{xy}$  surface is shown in Fig. 8. The "pull" on an infinitesimal fiber is proportional to the slope in the  $y$ -direction integrated along the  $x$ -direction. Note that the slope becomes infinite along the outer fibers at the wall.

It is of interest to compare the transverse displacements of the central fiber with those from Euler-Bernoulli beam theory with an added shear term using Cowper's results [6]†.

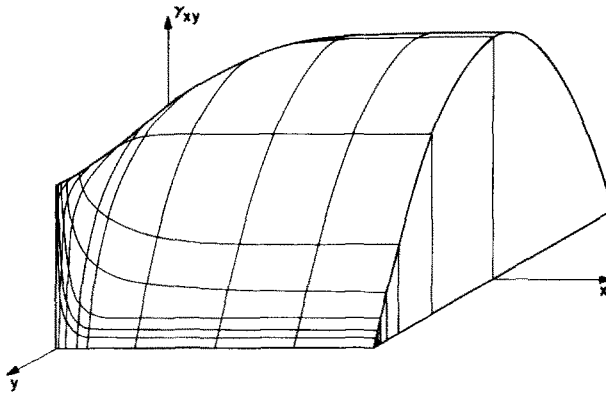


FIG. 8. Isometric view of  $\gamma_{xy}$  surface.

† It should be pointed out that displacement results were presented in [3] for a centrally loaded simply supported multilayer beam each half of which is equivalent to a cantilever beam with an unwarped end under the restrictions of the multilayer model. In the case of an elastic medium, there is a distinction between the cantilever and simply supported beam problems and the model approximates only the cantilever solution when the axial field is examined in detail.



In general there is little difference between the transverse deflections obtained with the present method in the case  $\sigma_y = 0$  and the Euler-Bernoulli theory with the added shear term. The numerical results for end deflection of the central fiber are given in tabular form below. Here  $\bar{v} = v/l$ .

TABLE 1. COMPARISON OF PRESENT RESULTS FOR END DEFLECTION WITH THOSE OBTAINED FROM THE EULER-BERNOULLI-COWPER SOLUTION

	$\eta$	$\bar{v} \times 10^4$		$\bar{v} \times 10^4$ Euler-Bernoulli-Cowper
		Equation (16) ... $\sigma_y = 0$	Equation (18) ... $\epsilon_y = 0$	
$\nu = 0$	2	1.060	1.060	1.067
	4	3.063	3.063	3.067
	10	17.065	17.065	17.067
$\nu = 0.3$	2	1.189	1.116	1.177
	4	3.195	2.941	3.177
	10	17.199	15.685	17.177

Data was also obtained for the transverse displacements of the outer fibers for the case  $\sigma_y = 0$ . The maximum difference between outer and central fiber deflections, which occurs at the wall, was generally very small, being less than one per cent of the end deflection for the long beam ( $\eta = 10$ ). Hence it would be reasonable to simplify the procedure for obtaining the transverse displacement by assuming  $v = v(x)$  and following the same procedure as in the  $\epsilon_y = 0$  case. This simplification is consistent with the others inherent in the model.

In Fig. 9 a comparison is made between the stress distribution obtained at the wall under each of the assumptions  $\sigma_y = 0$  and  $\epsilon_y = 0$ . The curve shown is a blow-up of the region near the outer surface where the deviation is most pronounced. Note that only the case for  $\nu = 0.3$  is shown because when  $\nu = 0$  both distributions are identical.

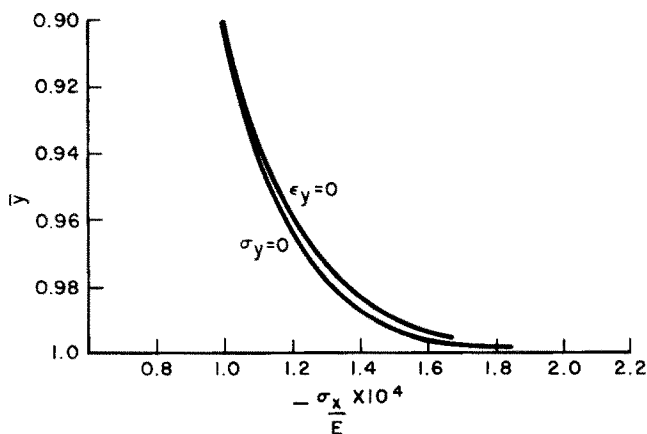


FIG. 9. Detail of stress distribution near wall corner  $\eta = 2, \nu = 0.3$ .

## DISCUSSION OF RESULTS FOR CANTILEVER BEAM

The assumptions made are coarse, and rule out the possibility of determining field information for the transverse direction. However, the field information obtained for the axial direction under the two alternate assumptions,  $\sigma_y = 0$  or  $\varepsilon_y = 0$ , is substantially the same in this example. That the transverse deflection predictions based on the  $\sigma_y = 0$  assumption are essentially in agreement with earlier estimates is gratifying. The mild discrepancies exhibited in the transverse deflections predicted under the  $\varepsilon_y = 0$  assumption are due to the unrealistic restraint imposed in this case which implies a stiffer Young's modulus [ $E/(1-\nu^2)$  vs.  $E$ ].

The model has also been applied to elastic layer problems. Comparisons to solutions from the exact theory have shown that the model yields reasonably accurate results for information in the direction of essential stresses even in areas where the zero transverse stress or strain assumptions would not seem applicable.

## CONCLUSIONS

Under appropriate assumptions the equations of isotropic elasticity yield a simple mathematical model which has been shown to give reasonable results for the beam example discussed. It is felt that in the type of problem for which the model is applicable the field information in the dominant direction is relatively insensitive to the particular coarse assumption made for the transverse direction. The ease with which this method can be applied to problems with rectangular boundaries justifies its consideration as a tool for obtaining estimates.

The model's apparent ability to describe end effects in beams is noteworthy. In place of the usual treatment of end boundary conditions in such problems in which only resultant forces and moments can be accommodated, with this model detailed normal stresses or displacements can be prescribed. End shear stress distributions, however cannot be prescribed arbitrarily. This is a limitation of the shear lag model which has previously been noted [7, 8].

The authors recently learned that the type of model discussed above, but with inertia forces added, was used by Budiansky and Kruszewski [9] in investigating the vibrations of hollow thin-walled beams and by Matuo and Ohara [10] in determining the lateral earth pressure on walls during earthquakes. However, because the simplifications used have not been generally popularized and the present journal is more readily available than the cited references it is felt that discussion of the model here is in order.

## REFERENCES

- [1] F. B. HILDEBRAND, The exact solution of shear-lag problems in flat panels and box beams assumed rigid in the transverse direction. NACA TN 894 (1943).
- [2] THEODORE VON KÁRMÁN and WEI-ZANG CHIEN, Torsion with variable twist. *J. aero. Sci.* **13**, 10, 503-510 (1946).
- [3] Y. M. TARNOPOLSKII, A. V. ROZE and V. A. POLYAKOV, Shear effects during bending of oriented glass-reinforced plastics. *Polymer Mech.* **1**, 2, 31-37 (1965).
- [4] T. J. P. A. BROMWICH, *Theory of Infinite Series*. 2nd Edition. Macmillan (1959).
- [5] M. L. WILLIAMS, Stress singularities resulting from various boundary conditions in angular corners of plates in extension. *J. appl. Mech.* **19**, 526-528 (1952).

- [6] G. R. COWPER, The shear coefficient in Timoshenko's beam theory. *J. appl. Mech.* **33**, 335–340 (1966).
- [7] E. REISSNER, Analysis of shear lag in box beams by the principle of minimum potential energy. *Q. J. appl. Math.* **4**, 268–278 (1946).
- [8] P. KUHN, *Stresses in Aircraft and Shell Structures*. McGraw-Hill (1956).
- [9] B. BUDIANSKY and E. T. KRUSZEWSKI, Transverse vibrations of hollow thin-walled cylindrical beams. NACA TR 1129 (1953).
- [10] H. MATUO and S. OHARA, Lateral earth pressure and stability of quay walls during earthquakes. Proceedings of the Second World Conference on Earthquake Engineering, Tokyo and Kyoto, Japan (1960).

(Received 12 December 1968; revised 11 September 1969)

**Абстракт**—Элементарная математическая модель, подобная к применяемой в анализе сдвига фаз и для описания преупругости континуума многослойного материала, используется для оценки решений задач, в рамках упругости изотропного тела, если предположить, что распределение напряжений или деформаций не зависит от направления. Эта модель принимается для случая консольной балки, нагруженной на конце, в которой не допущена деформация сечения в месте заделки. Поперечные прогибы хорошо согласуются с результатами теории Эйлера-Бернулли, при учете добавочной части от сдвига. В районах отдаленных от опоры, распределение осевых напряжений изменяется по линейному закону. Однако, сложные краевые эффекты определяются вблизи опоры ростом напряжений во внешних волокнах. Эти эффекты оказываются незначительными на небольшом расстоянии от опоры, согласно принципу де Сен-Венана.